Laser Doppler Velocimetry Measurements of A Turbulent Boundary Layer Flow over Sprayed Superhydrophobic Surfaces

James W. Gose

Department of Naval Architecture
and Marine Engineering
University of Michigan
2600 Draper Dr., Ann Arbor, MI 48109, USA
jgose@umich.edu

Kevin B. Golovin

Department of Materials Science and Engineering
University of Michigan
2800 Plymouth Rd., Ann Arbor, MI 48109
golovin@umich.edu

Julio M. Barros

Department of Mechanical Engineering
United States Naval Academy
590 Holloway Rd., Annapolis, MD 21402, USA
barros@usna.edu

Michael P. Schultz

Department of Naval Architecture
and Ocean Engineering
United States Naval Academy
590 Holloway Rd., Annapolis, MD 21402, USA
mschultz@usna.edu

Anish Tuteja

Department of Materials Science and Engineering
University of Michigan
2800 Plymouth Rd., Ann Arbor, MI 48103, USA
tuteja@umich.edu

Marc Perlin

Department of Naval Architecture
and Marine Engineering
University of Michigan
2600 Draper Dr., Ann Arbor, MI 48109, USA
perlin@umich.edu

Steven L. Ceccio

Department of Naval Architecture and Marine Engineering
University of Michigan
2600 Draper Dr., Ann Arbor, MI 48109, USA
ceccio@umich.edu

ABSTRACT

Measurements of near-zero pressure gradient turbulent boundary layer (TBL) flow over several superhydrophobic surfaces (SHSs) are presented and compared to those for a hydraulically smooth baseline. The surfaces were developed at the University of Michigan as part of an ongoing research thrust to investigate the feasibility of SHSs for skin-friction drag reduction in turbulent flow. The SHSs were previously evaluated in fully-developed turbulent channel flow and have been shown to provide meaningful drag reduction. The TBL experiments were conducted at the U.S. Naval Academy in a water tunnel with a test section 2.0 m (L) × 0.2 m (W) × 0.1 m (H). The free-stream speed was set to 1.25 ms^{-1}, nominally, which corresponded to a friction Reynolds number, Re_τ, of 1,600. The TBL was tripped at the test section inlet with a 0.8 mm diameter wire. The upper and side walls provided optical access, while the lower wall was either the smooth baseline or a spray coated SHS. The velocity measurements were obtained with a two-component Laser Doppler Velocimeter (LDV) and custom-designed beam displacer operated in coincidence mode. The LDV probe volume diameter was 45 μm (approx. two wall-units). The measurements were recorded 1.5 m downstream of the trip. When the measured quantities were normalized using inner variables, the results indicated a significant reduction in the near wall viscous and total stresses. Increased stresses were also measured in the overlap layer when compared to the smooth wall. Nevertheless, consideration of the total stress and a log layer with a wake analysis shows drag reduction of -11 to 36% for the SHS analyzed.

INTRODUCTION

Nature has provided an exhaustive source of evolutionary functional materials to be mimicked for everyday applications (Jung & Bhushan, 2010). One notable case relevant to the marine environment is the lotus leaf which is known for its self-cleaning properties and resistance to wetting (Neinhuis & Barthlott, 1997).

More specifically, lotus inspired superhydrophobic surfaces (SHSs) have been biomimetically developed for skin-friction reduction in various flow applications (Bhushan *et al.*, 2009; Samaha *et al.*, 2012). Exhaustively studied in small-scale laminar flows [see Rothstein (2010) for a review of SHS drag reduction and slip on SHSs], advances in the design and fabrication of SHSs has permitted application of these materials in more naval relevant flows.

A smooth surface can be characterized by its surface energy and the contact angle it makes with a drop of water. When the contact angle between a low surface energy material and a droplet exceeds 150 degrees, and maintains a low contact angle hysteresis $\Delta\theta$ (defined as the difference between the advancing θ_A and receding θ_R contact angles) the surface is classified as superhydrophobic. A large contact angle generally signifies a reduced wetted area and an ease of relative motion between the liquid/water and the underlying solid surface. Coupling this resistance to wetting with micro- and nano-scale roughness, a SHS can retain air pockets such that an air-liquid interface is maintained (where the liquid is water), which acts to reduce the local shear stress, τ_w, and may provide a slip length, λ_x, of approximately 10's μm. These physical properties provide a passive and potentially more efficient alternative to the traditional means of drag reduction, for example gas injection (i.e., air-layer, bubble, and partial-cavity drag reduction). Figure 1 shows a schematic representation of a SHS with an air-water interface and the associated idealized slip on the solid-liquid and air-liquid interfaces.

Previous SHS drag reduction studies, including but not limited to the work of Daniello *et al.* (2009), Ou *et al.* (2004), Ou & Rothstein (2005), Watanabe *et al.* (1999), Woolford *et al.* (2013), and Zhao *et al.* (2007), have shown the SHSs can reduce drag in laminar flow. However, application of such surfaces for skin-friction reduction in wall-bounded, high-Reynolds number, turbulent flows has been less successful. More specifically, SHS drag reduction has been limited to low-Reynolds number turbulent flows using small-scale, structured surfaces and large air-water interfaces (Daniello *et al.*, 2009; Henoch *et al.*, 2006; Park *et al.*, 2014), which can be unstable or become wetted in higher turbulence; or SHSs with small roughness scales, relative to the viscous length scale of the flow (Aljallis *et al.*, 2013; Bidkar *et al.*, 2014; Gose *et al.*, 2016; Ling *et al.*, 2016). Under other conditions Aljallis *et al.* (2013), Bidkar *et al.* (2014), Gose *et al.* (2016), Hokmabad & Ghaemi (2016), and Zhao *et al.* (2007) measured no change or a drag increase in the presence of a SHS. Tian *et al.* (2015) and Zhang *et al.* (2015) also measured skin-friction reduction of 10 and 24% respectively, in turbulent boundary layer (TBL) flows. The mixed results from this brief review brings to question both the effectiveness and mechanisms of superhydrophobic drag reduction in turbulent flows, and thus warrants further investigation, particularly for the application of SHS in large-scale, high-Re flows.

A group led by the University of Michigan, as part of a Multidisciplinary University Research Initiative, has developed a series of mechanically robust, spray superhydrophobic coatings that can be applied over significantly larger than are usually reported in SHS drag reduction studies, on the order of tens of square meters or more. This development is enhancing the understanding of the physics of flows along SHSs, and the potential for friction reduction in high-Reynolds number naval or mechanical hydraulic applications.

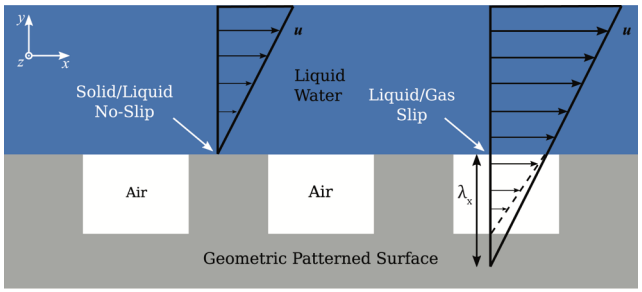

Figure 1. Idealized schematic representation of a geometrically patterned SHS with an intermittent slip/no-slip boundary conditions.

Our group has investigated several of these spray SHSs in a fully-developed turbulent flow channel measuring 1.20 m long, 0.10 m wide, and nominally 0.0073 m high (Gose *et al.*, 2016). The SHSs had contact angles exceeding 165° and maintained low-contact angle hysteresis (less than 3°), even after being exposed to flow for several hours. Using streamwise pressure drop along the channel, the skin-friction along the SHSs was inferred for friction Reynolds number ranging from 300 to 1000. The results showed that SHSs can provide sustainable friction reduction up to 50%, with the caveat that the SHS RMS roughness was less than the viscous length scale of the flow and that the surface had a strong resistance to wetting.

In this paper we will discuss the fabrication and experimental evaluation of six spray SHSs, and summarize the analysis methods used for mean flow field and skin-friction characterization for comparison to a hydrodynamically smooth baseline surface. This discussion will focus on the application and efficacy of the SHSs in an external TBL flow.

SUPERHYDROPHOBIC SURFACE DESCRIPTION

We have fabricated several SHSs that provide drag reduction in turbulent flow that have been previously described by Gose *et al.* (2016) and Golovin *et al.* (2017). Additional surface variations of the coatings were generated to evaluate the effective roughness for coatings with the same surface chemistry. A brief discussion of the SHS fabrication is proved here-in.

Surface 1 (1A through 1D) was fabricated by spray coating a blend of a fluorinated polyurethane polyol (Helicity Inc.) with a highly hydrophobic molecule, fluorodecyl polyhedral oligomeric silsesquioxane (F-POSS). A solution of the polyol and a urethane crosslinker, 4,4′-Diisocyanato-methylenedicyclohexane (Wanhua Chemical Group Co.), was dissolved in Vertrel XF (Chamois). To this solution, the F-POSS was added such that the overall concentration was 200 mg per mL and 20 wt% was comprised of the F-POSS. The mixture was sonicated until it became completely transparent, approximately 30 seconds. Volumes of 10 ml (1C), 20 ml (1A,1B), and 40 ml (1D) of the solution were sprayed onto a 1.2 m x 0.2 m polycarbonate substrate using an ATD Tools 6903 high volume-low pressure spray gun with compressed air at a pressure of 140 kPa (20 psi). The sample was cured at 80 degrees

C for 72 hours in an ambient environment using a silicone heating pad. An SEM image of Surface 1D is shown in Figure 2.

Surface 2 was fabricated by forming a solution of fast-curing superglue (SF-100, 3M) and the same F- POSS molecules as above in equal mass fractions in Asahiklin-225 (Asahi Glass Co.) at a concentration of 50 mg per mL. The solution was sprayed using the same procedures as Surface 1. Surface 2 was cured at 50 degrees C for 60 minutes. An SEM image of Surface 2 is shown in Figure 2.

Surface 3 consisted of a blend of the fluorinated polyurethane polyol and crosslinker from Surface 1 and fluoro-functionalized silica nanoparticles. The particles are nominally 50 to 100 nm irregular aggregates, the synthesis of which is described by Campos e*t al.* (2011). A 25 mg per mL solution of these components was formed in Vertrel XF, with 35% of the total mass being the silica particles. A total of 20 mL of this solution was sonicated until clear, and then sprayed and cured using the same procedures as for Surface 1. It is important to note that this surface derives its roughness from the silica nanoparticles, as opposed to the spraying process as with surfaces 1 and 2, and in this way the roughness could be kept small compared to the other sprayed surfaces.

Samples of the coatings were used to characterize the SHSs' roughness and wettability prior to testing. A Philips XL30 FEG scanning electron microscope was used to image the surfaces and surface profilometry was performed using an Olympus LEXT interferometer. Using a step size of 1.25 μm and an overall scan area of 2.50 mm × 2.50 mm, the two-dimensional root-mean-square roughness S_q, as defined in Eq. (1), was computed and averaged for the three areas.

$$S_q = \sqrt{\frac{1}{A}\iint_A Z^2(x,y)\,dx\,dy} \tag{1}$$

In Eq. (1), A is the area being characterized and Z is the height of the surface at point (x, y). S_q was systematically varied from 1.7 ± 0.3 μm to 33 ± 4 μm for the samples tested, which will provide critical insight into the effect of superhydrophobic roughness when exposed to turbulent flow.

EXPERIMENTAL SETUP

Experiments were conducted in a recirculating water tunnel designed for detailed boundary-layer measurements. The test section was 2.0 m long, 0.2 m wide, and nominally 0.1 m high. The bottom wall was a flat plate which served as the test wall. The upper wall was adjustable and set for a zero streamwise pressure gradient with a nominal free-stream velocity, U_0, of 1.25 ms^{-1} for all cases. The acceleration parameter, defined as

$$K = \frac{\nu}{U_0^2}\frac{dU_0}{dx} \tag{2}$$

was less than 5×10^{-9}. The upper wall and sidewalls provided optical access. The boundary-layer was tripped near the leading edge with a 0.8 mm diameter wire, fixing the location of transition and ensuring a TBL over the surfaces. Velocity measurements

Table 1. Summary of the two-dimensional root-mean-square roughness S_q, as defined in Eq. (1).

Surface	1A	1B	1C	1D	2	3
S_q [μm]	22±1	24±2	16±2	33±4	1.9±0.2	1.7±0.4

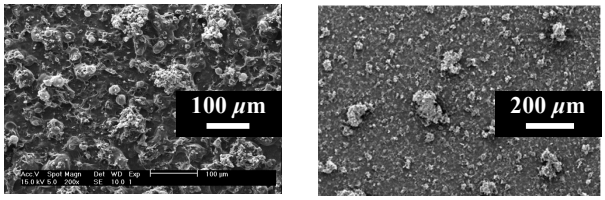

Figure 2. SEM micrographs of Surface 1D (left) and 2 (right).

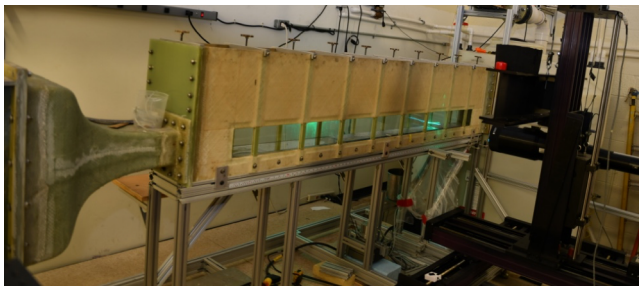

Figure 3. Image of the recirculating TBL facility that was used in this work. The facility is located at the U.S. Naval Academy and has been used in numerous TBL experiments by Drs. Michael Schultz and Karen Flack. The LDV system is shown on the right, while the SHS is seen in the bottom wall of the facility.

showed that a core flow remained at downstream end of the test section. Flow was supplied to the test section from a 4,000 L cylindrical tank. Water was drawn from the tank by two variable-speed, 7.5 kW pumps operating in parallel, and then sent to a flow-conditioning section consisting of a diffuser containing perforated plates, a honeycomb, three screens and a three-dimensional contraction. The test section immediately followed the contraction. The free-stream turbulence level was less than 0.5%. Water exited the test section through a perforated plate emptying into the cylindrical tank. The test fluid was filtered and deaerated water. A chiller was used to keep the water temperature constant to within one Kelvin during all tests.

Boundary-layer velocity measurements were obtained with a TSI FSA3500 two-component laser Doppler velocimeter (LDV). The LDV consists of a four-beam fiber optic probe that collects data in backscatter mode. A custom-designed beam displacer was added to the probe to shift one of the four beams, resulting in three co-planar beams that can be aligned parallel to the wall. Additionally, a 2.6:1 beam expander was located at the exit of the probe to reduce the size of the measurement volume. The resulting probe volume diameter, d, was 45 μm with a probe volume length (l) of 340 μm. The corresponding measurement volume diameter and length in viscous length scales were $d^+ \leq 2.2$ and $l^+ \leq 16$.

Measurements were recorded approximately 1.5 m downstream of the trip, or 0.8 m downstream of the leading edge of the SHS plates resulting in development length of approximately

Table 2. Summary of the flow parameters from the total stress method, adopted and modified from Ling *et al.* (2016).

Surface	U_0 [ms^{-1}]	δ [mm]	u_τ [ms^{-1}]	Re_τ [ ]	C_f [10^{-3}]	DR [%]
Smooth wall	1.24	33.5	0.046	1626	2.80	-
1A	1.27	34.3	0.040	1442	2.00	+28
1B	1.26	33.5	0.041	1446	2.15	+23
1C	1.29	30.9	0.046	1491	2.56	+8.3
1D	1.29	27.9	0.045	1328	2.47	+12
2	1.26	35.8	0.041	1542	2.13	+24
3	1.28	34.1	0.038	1363	1.79	+36

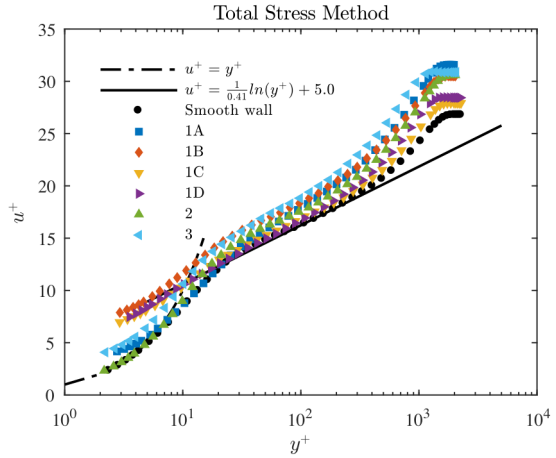

Figure 4. Mean velocity profiles for the hydrodynamically smooth baseline and the SHSs - non-dimensionalized by the smooth wall data as determined from the total stress method - at nominal Re_τ of 1,600.

45δ (boundary layer height). For the velocity profiles, the LDV probe was traversed to 45 locations within the boundary layer with a Velmex three-axis traverse unit. The traverse allowed the position of the probe to be maintained to ±5 μm in all directions. For the first 10 points near the wall, a total data sampling time was set to 300 seconds, yielding ~10,000 to 20,000 random velocity samples for each velocity component. The large sampling time was necessary for the velocity statistics to converge, due to the lower data rate in the near-wall region. Subsequent points were limited to 180 seconds for sake of time, however, yielding ~30,000 or more data point per wall-normal location. The experiments were conducted over the period of approximately four hours. The data were collected in coincidence mode. The flow was seeded with 2 μm diameter silver-coated glass spheres.

EXPERIMENTAL RESULTS

In the following sections we discuss the mean velocity profile and stresses as determined from two analysis methods: the total stress method, similar to Ling *et al.* (2016), and a new method which used a log+wake fit to the velocity profile. The analysis method directly affects the outcome of the local shear stress, and

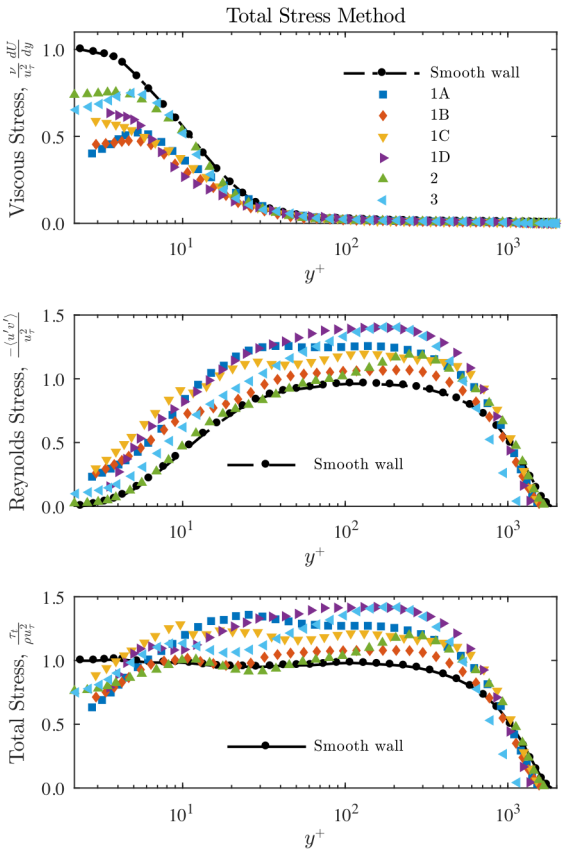

Figure 5. Profiles of the viscous shear stress, Reynolds stress, and total shear stress for the hydrodynamically smooth baseline and the SHSs - non-dimensionalized by the smooth wall data as determined from the total stress method - at nominal Re_τ of 1,600.

in turn, the resulting drag reduction as defined in Eq. (4), where C_f is the coefficient of skin-friction.

$$DR = \frac{C_{f,Smooth} - C_{f,SHS}}{C_{f,Smooth}} \quad (4)$$

Total Stress Method

A method based on the total shear-stress, similar to Ling *et al.* (2016) was implemented, and its performance tested. Mean velocity profiles are presented in Figure 4, while the stresses, non-dimensionalized the smooth wall friction velocity, u_τ, are shown in Figure 5. The total stress method uses an average of the first five points in the total stress to determine the wall shear stress and friction velocity. We believe this is a conservative estimate based on the shape of the stresses in Figure 5, which do not asymptote to one. Table 2 summarizes the flow parameters as determined from the total stress method with DR ranging from +8 to +36% for the six SHS discussed.

The mean velocity profiles for the SHSs had an increase velocity from wall through the wake region of the TBL. The increase in the mean velocity profiles is likely due to the presence of the air-water interface, and indicated that the roughness of the SHSs is not negatively affecting the flow and that an overall drag

Table 3. Summary of the flow parameters from the log+wake method defined in Eq. (3).

Surface	U_0 [ms^{-1}]	δ [mm]	u_τ [ms^{-1}]	Re_τ [ ]	C_f [10^{-3}]	DR [%]
Smooth wall	1.24	33.5	0.046	1620	2.77	-
1A	1.27	34.3	0.050	1789	3.09	-11
1B	1.26	33.5	0.043	1510	2.34	+16
1C	1.29	30.9	0.043	1386	2.22	+20
1D	1.29	27.9	0.049	1424	2.84	-2.3
2	1.26	35.8	0.042	1564	2.20	+21
3	1.28	34.1	0.047	1693	2.76	+0.5

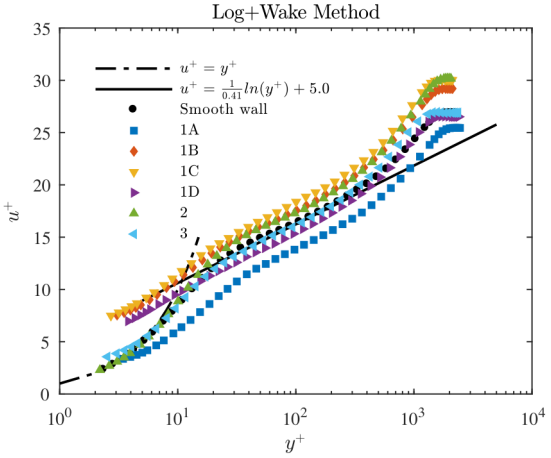

Figure 6. Mean velocity profiles for the hydrodynamically smooth baseline and the SHSs - non-dimensionalized by the smooth wall data as determined from the log+wake method - at nominal Re_τ of 1,600.

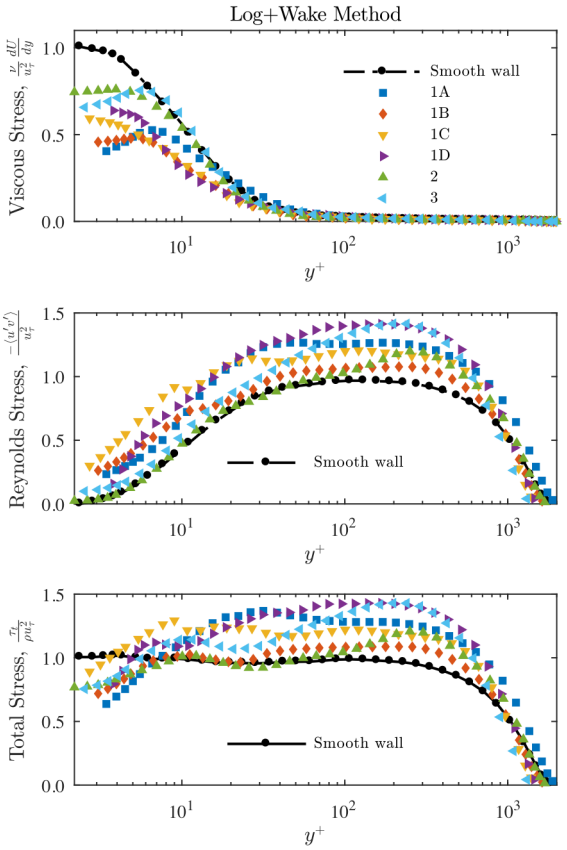

Figure 7. Profiles of the viscous shear stress, Reynolds stress, and total shear stress for the hydrodynamically smooth baseline and the SHSs - non-dimensionalized by the smooth wall data as determined from the log+wake method - at nominal Re_τ of 1,600.

reduction is expected, particularly considering the viscous length scale was a fraction of the roughness of the SHSs evaluated. Moreover, the stresses indicate decrease in the near wall viscous stress of 25 to 50% for each of SHS with an increase of near-zero to 25% in the near-wall Reynolds stresses. The increases in Reynolds stress generally appear to coincide with increases in roughness. Lastly, from the stresses it is very apparent that increases in both u' and v' over the smooth wall result in significantly higher Reynolds stress and total stress in the overlap region of the TBL.

Although not presented here, the total stress method was verified to produce widely different C_f estimations on multiple runs from the same SHS surface. One possible explanation is that small changes in pressure drag could occur due to the local plastron topography where the LDV measurements were taking place. This may have introduced concomitant changes in both viscous and Reynolds shear stress in the sublayer region, and thus affect the C_f estimation from the total stress profile.

Log+Wake Method

Because the LDV measurements were taken several boundary layer thicknesses downstream of the leading edge of the SHSs, the flow could adjust to a new, drag reducing self-similar state. Therefore, the log-layer should reflect, in a mean sense, the structural changes due to the new wall boundary condition. Therefore, to determine the wall shear stress, and thus the friction velocity and C_f, a nonlinear least square minimization based on the logic of a log-law plus wake deviation for rough-wall flows was implemented, in the form

$$U^+ = \frac{1}{\kappa}\ln\left(y^+\right) + B + \frac{2\Pi}{\kappa}\sin^2\left(\frac{y}{\delta}\frac{\pi}{2}\right) - \Delta U^+ \qquad (3)$$

where $\kappa = 0.41$ and $B = 5$ are the smooth wall log-law values, and u_τ, ΔU^+ and $\prod$ are the parameters determined from the nonlinear minimization. For the SHS, a negative ΔU^+ means that the shift in the log-law is above the smooth-wall log-law resulting in drag reduction.

Table 3 summarizes the flow parameters for the log+wake method. Mean velocity profiles are presented in Figure 6, while the stresses, non-dimensionalized the smooth wall friction velocity, u_τ, are shown in Figure 7. Although the non-dimensionalized stresses look very similar to the results from the total stress method, the mean velocity profiles of the SHSs have greater variation when

compared to the smooth wall. Most notably, the SHS have velocity profiles that lie both above and below the smooth wall data, yet all of the SHS result in local *DR* ranging from -11 to +21%. This result is a bit surprising as a reduction in u^+ is consistent with the presences of a rough surface in a TBL. Nevertheless, unlike the total stress method, consistent estimation of the friction velocity was seen from multiple runs for a given tested SHS when analyzed using the log+wake method.

CONCLUSION

In this brief review, we have highlighted the need to further investigate SHS for turbulent drag reduction in large-scale applications. The surfaces were designed to be a scalable spray formulation with strong mechanical durability and resistance to wetting. The result previously collected and shown here for an external TBL flow at friction Reynolds number are in good agreement. These results will be further explored with additional data to further validate the application of SHSs for an advantageous modification of the flow field in the vicinity of wall-bounded flows. The aforementioned discussion emphasizes the importance of analysis methods used to characterize flow field and skin-friction in turbulent flow. As shown here, two methods used to characterize frictional benefits of SHS can provide very different results. Nevertheless, it is believed the spray SHSs discussed here were appropriated designed and applied to provided meaningful (>10%) *DR* in naval relevant, TBL flows.

ACKNOWLEDGEMENTS

This project was carried out as part of the U.S. Office of Naval Research (ONR) MURI (Multidisciplinary University Research Initiatives) program (Grant No. N00014-12-1-0874) managed by Dr. Ki-Han Kim and led by Dr. Steven L. Ceccio.

REFERENCES

Aljallis, E., Sarshar, M. A., Datla, R., Sikka, V., Jones, A., & Choi, C. H. 2013. Experimental study of skin friction drag reduction on superhydrophobic flat plates in high Reynolds number boundary layer flow. *Physics of Fluids*, *25*, 25103.

Bhushan, B., Jung, Y. C., & Koch, K. 2009. Micro-, nano- and hierarchical structures for superhydrophobicity, self-cleaning and low adhesion. *Philosophical Transactions. Series A, Mathematical, Physical, and Engineering Sciences*, *367*, 1631–1672.

Bidkar, R. A., Leblanc, L., Kulkarni, A. J., Bahadur, V., Ceccio, S. L., & Perlin, M. 2014. Skin-friction drag reduction in the turbulent regime using random-textured hydrophobic surfaces. *Physics of Fluids*, *26*, 85108.

Campos, R., Guenthner, A. J., Haddad, T. S., & Mabry, J. M. 2011. Fluoroalkyl-functionalized silica particles: Synthesis, characterization, and wetting characteristics. *Langmuir*, *27*, 10206–10215.

Daniello, R. J., Waterhouse, N. E., & Rothstein, J. P. 2009. Drag reduction in turbulent flows over superhydrophobic surfaces. *Physics of Fluids*, *21*. doi:10.1063/1.3207885

Golovin, K., Boban, M., Mabry, J. M., & Tuteja, A. 2017. Designing Self-Healing Superhydrophobic Surfaces with Exceptional Mechanical Durability. *ACS Applied Materials & Interfaces*, *9*, acsami.6b15491.

Gose, J. W., Golovin, K., Tuteja, A., Ceccio, S. L., & Perlin, M. 2016. Experimental Investigation of Turbulent Skin-Friction Drag Reduction Using Superhydrophobic Surfaces. In *31st Symposium on Naval Hydrodynamics*. Monterey, CA.

Henoch, C., Krupenkin, T. N., Kolodner, P., Taylor, J. A., Hodes, M. S., Lyons, A. M., … Breuer, K. 2006. Turbulent drag reduction using superhydrophobic surfaces. In *Collection of Technical Papers - 3rd AIAA Flow Control Conference* (Vol. 2, pp. 840–844). San Francisco, CA, USA.

Jung, Y. C., & Bhushan, B. 2010. Biomimetic structures for fluid drag reduction in laminar and turbulent flows. *Journal of Physics: Condensed Matter*, *22*, 35104.

Ling, H., Srinivasan, S., Golovin, K., McKinley, G. H., Tuteja, A., & Katz, J. 2016. High resolution velocity measurement in the inner part of turbulent boundary layers over super-hydrophobic surfaces. *Journal of Fluid Mechanics*, *accepted*, 670–703.

Neinhuis, C., & Barthlott, W. 1997. Characterization and Distribution of Water-repellent, Self-cleaning Plant Surfaces. *Annals of Botany*, *79*, 667–677.

Ou, J., Perot, B., & Rothstein, J. P. 2004. Laminar drag reduction in microchannels using ultrahydrophobic surfaces. *Physics of Fluids*, *16*, 4635–4643.

Ou, J., & Rothstein, J. P. 2005. Direct velocity measurements of the flow past drag-reducing ultrahydrophobic surfaces. *Physics of Fluids*, *17*, 103606.

Park, H., Sun, G., & Kim, C.-J. "CJ." 2014. Superhydrophobic turbulent drag reduction as a function of surface grating parameters. *Journal of Fluid Mechanics*, *747*, 722–734.

Rothstein, J. P. 2010. Slip on Superhydrophobic Surfaces. *Annu. Rev. Fluid Mech*, *42*, 89–109.

Samaha, M. A., Tafreshi, H. V., & Gad-el-hak, M. 2012. Colloids and Surfaces A : Physicochemical and Engineering Aspects Effects of hydrostatic pressure on the drag reduction of submerged aerogel-particle coatings. *Colloids and Surfaces A: Physicochemical and Engineering Aspects*, *399*, 62–70.

Tian, H., Zhang, J., Wang, E., Yao, Z., & Jiang, N. 2015. Experimental investigation on drag reduction in turbulent boundary layer over superhydrophobic surface by TRPIV. *Theor. Applied Mech. Letters*, *5*, 45–49.

Vajdi Hokmabad, B., & Ghaemi, S. 2016. Turbulent flow over wetted and non-wetted superhydrophobic counterparts with random structure. *Physics of Fluids*, *28*, 15112.

Watanabe, K., Udagawa, Y., & Udagawa, H. 1999. Drag reduction of Newtonian fluid in a circular pipe with a highly water-repellent wall. *Journal of Fluid Mechanics*, *381*, 225–238.

Woolford, B., Prince, J., Maynes, D., & Webb, B. W. 2009. Particle image velocimetry characterization of turbulent channel flow with rib patterned superhydrophobic walls. *Physics of Fluids*, *21*, 5106.

Zhang, J., Tian, H., Yao, Z., Hao, P., & Jiang, N. 2015. Mechanisms of drag reduction of superhydrophobic surfaces in a turbulent boundary layer flow. *Experiments in Fluids*, *56*, 1–13.

Zhao, J. P., Du, X. D., & Shi, X. H. 2007. Experimental research on friction-reduction with super-hydrophobic surfaces. *Journal of Marine Science and Application*, *6*, 58–61.